Archives of Environmental Protection
Vol. 47 no. 1 pp. 3–9

PL ISSN 2083-4772
DOI 10.24425/aep.2021.136442

Phosphorus removal by microelectrolysis and sedimentation in the integrated devices

Bartosz Libecki, Tomasz Mikołajczyk*

Department of Chemistry, Faculty of Environmental Management and Agriculture,
University of Warmia and Mazury in Olsztyn, Poland

*Corresponding author's e-mail: tomasz.mikolajczyk@uwm.edu.pl

Keywords: ZVI, phosphorus removal, microelectrolysis, coagulator

Abstract: This paper presents the results of tests performed on an installation with an aerated microelectrolytic bed (MEL-bed) and sludge sedimentation. The systems were designed in two versions, differing in the aeration method, i.e., a mechanically aerated coagulator (MAC) and an automatically aerated coagulator (AAC). The experiment demonstrated a high (approx. 84%) efficiency of phosphorus removal from a model solution for both versions. The corroding bed was the source of iron in the solution. In the initial phase aeration method affected the phosphorus removal rate, flocculation and sedimentation processes. Physical and chemical changes in the MEL-bed packing were observed.

Introduction

Phosphorus (apart from nitrogen) is the main agent limiting the eutrophication of water bodies (Sterner 2008; Tarkowska-Kukuryk 2013). Restrictive standards concerning the quality of wastewater discharged into natural water bodies are being imposed (Gromiec and Gromiec 2010). It is possible to obtain the assumed permissible concentrations for phosphorus in wastewater discharged from wastewater treatment plant after applying either biological dephosphatation or chemical precipitation methods using coagulants, i.e., aluminium or iron(III) salts (Gu et al. 2011; Zou and Wang 2017). Chemical coagulation is also initiated by the dissolution of metals in the electrocoagulation process after an electric current was applied to the electrodes (Smoczyński et al. 2014). A source of metals in the solution may also be a galvanic cell built of electrodes of steel (anode) and carbon (cathode), immersed in an electrolyte (Yuan et al. 2009). As a result of microelectrolysis processes, during the contact of the bed with electrolyte, i.e., wastewater, steel corrosion takes place. The high degree of steel fragmentation guarantees a large specific surface area of the bed and, thus, a countless number of corrosion spots, i.e., micro-cells in which cathodic and anodic processes take place. In the anodic zone, oxidation and the release of electrons and metal cations take place, while a reduction occurs on the cathode (Yang 2009). Fe^{2+} cations released as a result of the steel bed disintegration are a substrate for further processes with the production of hydrolysis products, i.e., iron(III) hydroxycations that are capable of destabilizing colloids with an opposite charge, and hydroxides that are capable of adsorbing contaminants (Deng et al. 2013).

The effect of corrosive dissolution of iron in the form of chips or filings as Fe^0 (zero-valent iron – ZVI) for wastewater treatment has been presented in numerous studies (Sun et al. 2016),which indicate that the most important factors affecting the rate of corrosion processes include the type and surface of the steel, the presence of dissolved oxygen, electrolytic conductivity, the pH and the electrolyte composition.

There are many examples of new wastewater treatment installations using a microelectrolytic bed to streamline this process. The ZVI method with a bed in the form of immersed steel chip packs with the addition of 0.1% Cu was applied for a full-scale municipal wastewater treatment (Ma and Zhang 2008) to enhance the process. The above was obtained thanks to higher standard potential of copper compered to iron. Constant wastewater flow through the steel bed and infiltration ensured continuous microelectrolysis process and contact with the electrolyte. The process can be intensified under aerobic conditions, e.g., as a result of forced aeration of wastewater with a fine bubble aerator placed below the bed pack (Qin et al. 2011; Yanhe et al. 2016).

The advantages of this treatment method over the traditional chemical coagulation may be due to the following:

- Availability of raw materials – the opportunity to utilize waste materials (steel scrap);
- Elimination of secondary contamination – chemical coagulation leads to an increase in salinity and a decrease in the pH value;
- Minimization of the environmental impact – a reduction in energy and environmental hazards associated with the production of acidic coagulants (chemical processes associated with the emission of chemicals into the

environment) as well as the storage and transport of hazardous cargo.

The study aimed to test phosphate removal using a microelectrolytic bed operating under aerobic conditions with sludge separation by the sedimentation method at a new integrated wastewater treatment installation.

Experimental

Description of the devices tested

For the study, two versions of self-made based on a patent application (Libecki 2018) wastewater treatment coagulators were tested, one with mechanical aeration (Fig. 1, MAC) and the other one with automatic aeration (Fig. 2, AAC). The treatment process was initiated in the reaction tank, at the bottom of which the microelectrolytic bed (MEL-bed) was packed in the form of steel chips < 2 mm in size from unalloyed carbon steel with a weight of 3 g. Steel chips were initially degreased in 0.1 M NaOH, then rinsed with distilled water and dried.

The experiment was carried out on a laboratory scale for a model solution with characteristics provided in Table 1. 150 cm^3 of the solution was placed in the outer tank |1| of the coagulator (Fig. 1 and Fig. 2) and forced with a pump |7| with a flow rate of 5 cm^3/min through a suction flange |8| and the conduit terminated with a nozzle |9| in the reaction tank |3| with a capacity of 5 cm^3. The aerated solution under pressure penetrated through the steel bed and, along with the reaction products, escaped via the holes in the upper part of the reaction tank into the inner tank |2|. In the inner tank, the first separation of the post-coagulation sludge suspensions took place, and the solution overflowed through the upper edge of the tank into the outer tank |1|. For the MAC coagulator, the solution was aerated using an aerator |6| with a constant capacity of 5 cm^3 air/min. On the other hand, the AAC coagulator was equipped with a system of perforated PE flanges through which the solution was cascading.

The arangment of reactors – the total volume of tank (Vt) and retention time (Tr)

Outer tank |1| (glass cylinder) Vt – 400 cm^3, Tr – 21 min; Inner tank |2| (polyethylene cylinder) Vt – 45 cm^3, Tr – 8 min.; Reaction tank |3| (polyethylene container) 5 cm^3, Tr – 60 s; MEL-bed |4| V – 1,5 cm^3, Tr – 18 s.

Analytical methods

Tests of MEL-bed coagulators were carried out using solutions with and without phosphates (Table 1). During the experiment without PO_4^{3-} added, the corrosion performance of the steel bed was analysed by testing for the Fe^{3+} concentration, pH and electrolytic conductivity in the solution from the outer tank. After the completion of the experiment with a phosphate-free solution, the precipitated sludge was drained (on cellulose filter paper with pore size 12 mm) and dried at 100°C to a constant weight. During the test with phosphates added, the PO_4^{3-} concentration was analysed in the solution from the outer tank. At 30 min intervals, a sample of the solution was taken for tests and supplemented with the initial solution. For the measurements, a pH-meter and a conductometer with a conductivity probe (HANNA Instruments) were used. The concentration of Fe^{3+} was determined using the thiocyanate colorimetry (quantification limit of this method was on the level of 0.2 mg Fe^{3+}/dm^3), while PO_4^{3-} concentration by the molybdate method (quantification limit of this technique was on the level of 0.3 mg) (HACH). Additionally, spectroscopic characterization and elemental composition of the bed filling surface were performed by means of Quanta FEG 250 Scanning Electron Microscope (SEM), equipped with an Energy-Dispersive X-ray Spectroscopy (EDX) supplement (Bruker XFlash 5010). EDX tests were carried out at an acceleration voltage of 12 kV.

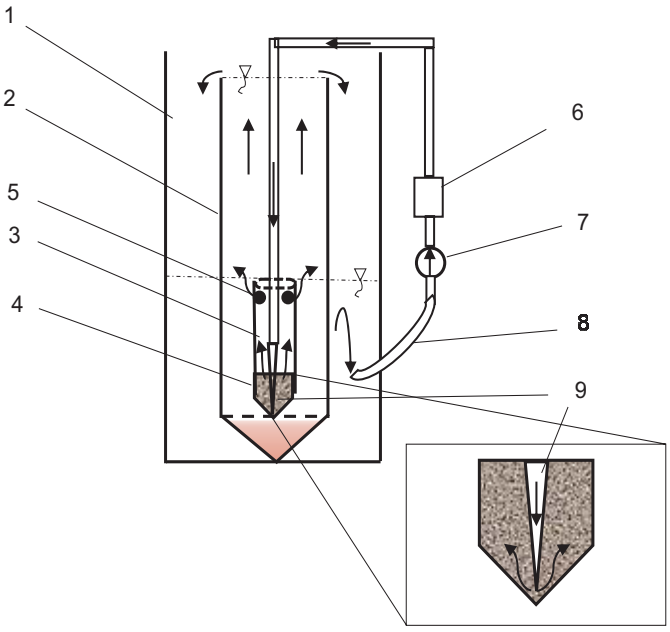

Fig. 1. Mechanically aerated coagulator (MAC)
1 – Outer tank, 2 – inner tank, 3 – reaction tank, 4 – MEL-bed, 5 – drain holes, 6 – aerator, 7 – circulating pump, 8 – pump suction flange, 9 – conduit terminated with a nozzle

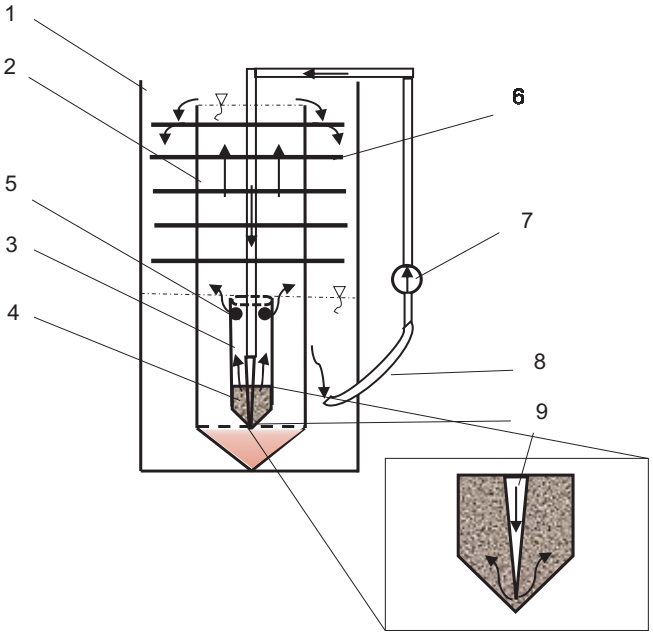

Fig. 2. Automatically aerated coagulator (AAC)
1 – Outer tank, 2 – inner tank, 3 – reaction tank, 4 – MEL-bed, 5 – drain holes, 6 – aerating rings, 7 – circulating pump, 8 – pump suction flange, 9 – conduit terminated with a nozzle

Results and discussion

Figures 3a and 3b show changes in the solution parameters during the experiment. In both cases, similar changes, such as an increase in the pH value and a decrease in conductivity were observed.

The coagulators were operating in aerobic conditions. Within the volume of the corrosive bed, the electrolysis process took place, which can be divided into anodic and cathodic parts. As a result of the anodic oxidation, Fe^{2+} ions are released from the steel. During the cathodic reduction under aerobic conditions and in a neutral pH, alkalization of the environment takes place in the carbon inclusion sites:

$$2Fe - 4e^- \rightarrow 2Fe^{2+}$$

$$O_2 + 2H_2O + 4\,e^- \rightarrow 4OH^-$$ (Yang et al. 2009).

At the same time, the conductivity decreases probably due to reactions of the solution components, i.e., hydrolysis and precipitation, the visible effect of which is the formation of sediment at the bottom of the inner tank. The inhibition of conductivity changes after 120 minutes is associated with the alkalization and the establishment of the chemical equilibrium of the occurring processes of steel bed dissolution and iron(II) ion hydrolysis (Sarin et al. 2004; Yang et al. 2017). In a weak alkaline environment, phosphates are bound by Fe oligomeric species (El Samrani et al. 2004).

Changes in the iron(III) ions concentration in the solution in Figs. 4a and 4b indicate the progress of corrosion processes. An effect of the operation of the system was the Fe(III) concentration at a level of 2–2.5 mg Fe^{3+}/l for the MAC system, and 1.5–2 mg Fe^{3+}/l for the AAC. The mechanical aeration method probably more efficiently intensifies the electrode processes involving oxygen reduction by accelerating the bed corrosion and the ferrous oxidation to ferric hydroxides and oxides (Wei et al. 2011; Lakshmanan et al. 2009).

After the contact with the corrosion bed, wastewater along with the iron hydrolysis products was flowing out through the holes in the upper part of the reaction tank into the inner container, where the further stage of floccule growth, separation of easily-settling suspensions and sedimentation took place. The total weight of sludge in the installation, determined after 6 h of the experiment with no phosphates, came to 4 and 8 mg for the MAC and AAC, respectively. These results indicate a high content of a large amount of suspended matter in the system. Heavy aeration may adversely affect the processes of floccule growth and fragmentation and problems with the sedimentation. As a final result, the treatment efficiency may be limited. Therefore, the technology using a microelectrolytic bed with aeration should assume the final filtration process.

At the same time, a reduction in phosphate concentration (Fig. 4) was observed and after 300 minutes of the experiment reached a value of 4.80 mg PO_4^{3-}/l in both tested systems. The phosphate removal rate (V_r) changed throughout the investigations (Fig. 5). In both cases, the value of V_r parameter was increasing with time till 30th min of the experiment when it reached its maximum value of 0.40 mg PO_4^{3-}/min for the MAC, compared to only 0.26 mg PO_4^{3-}/min for the AAC. After 30 min, the V_r parameter value was progressively decreasing at a different rate. Consequently, the final effectiveness after 300 minutes of the experiment was the same for both coagulators. The effect of aeration may be of fundamental importance to the course of phosphorus removal kinetics in the initial phase of the process. The process can proceed as a result of phosphate precipitation in accordance with the following reaction:

$$3Fe^{2+} + 2PO_4^{3-} + 8H_2O \rightarrow Fe_3(PO_4)_{2\downarrow},$$

with the minimum solubility of the precipitated products at pH of 7–8 (Priambodo et al. 2018). After 30 minutes, the phosphate

Table 1. Characteristics of the model solution

pH	Conductivity mS/cm	HCO_3^- mg/L	Cl^- mg/L	SO_4^{2-} mg/L	PO_4^{3-} mg/L	Na^+ mg/L	K^+ mg/L	Ca^{2+} mg/L
1	2	3	4	5	6	7	8	9
7.6	640	122	71	48	30	69	12	40

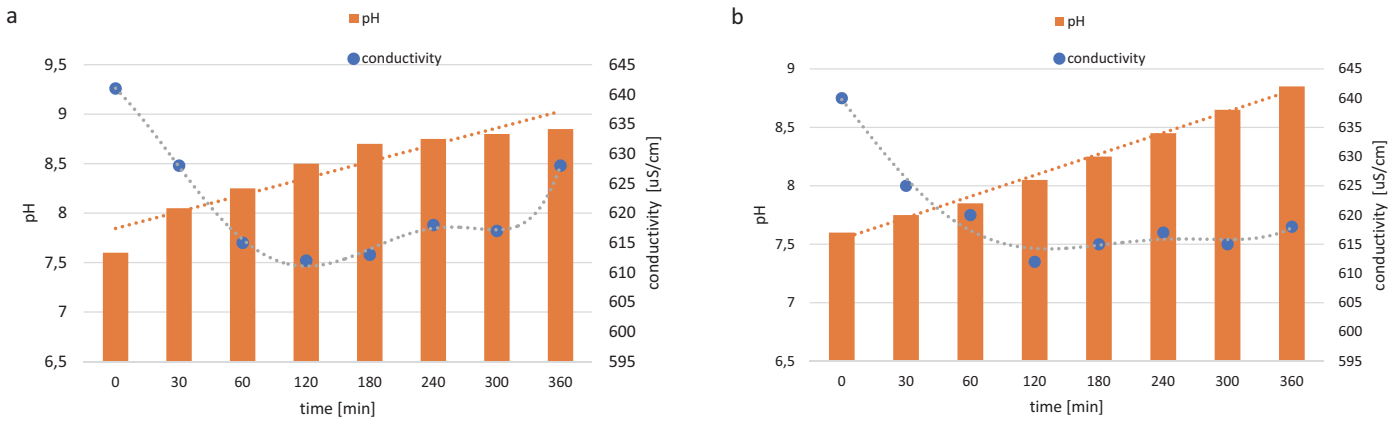

Fig. 3. Changes in the solution pH and conductivity during the experiment: a – MAC, b – AAC

removal efficiency decreases rapidly at pH of already above 8. This is associated with the substrate depletion, but also with the change in process conditions, i.e., an increase in pH and oxygenation. Under the influence of oxygen, the reactions of Fe(II) oxidation → Fe(III) and the hydrolysis with $Fe(OH)_3\downarrow$ precipitation are intensified. OH^- ions compete with PO_4^{3-} for Fe^{3+} ions and, at the same time, sorption processes can proceed (Li et al. 2009). Smoczyński et al. (2014) found that the main mechanism of phosphorus removal in the chemical and electrochemical coagulation processes is the chemical sorption process (chemisorption); as a result, covalent bonds are formed between the adsorbate particles and the adsorbent – hydrolysed metal species surface.

Comparing the bed structure from the SEM/EDX image before the experiment (Fig. 6a) and after 6 hours of the process (Fig. 6b), a significant increase in the surface roughness can be observed. These changes are the effect of the steel bed dissolution and adsorption of dissolved compounds and hydrolysis products in the form of incrustation on the surface. An elementary analysis of the surface granule layer of the bed before electrolysis (Fig. 7 and Table 2) revealed a composition typical to carbon steel with a Fe content of approx. 70% and carbon content of 20% along with the additions of Al and Mn, and traces of Si and Cu. After the electrolysis process (Fig. 8 and Table 3), the total share of iron and carbon decreased by approx. 10% and 6%, correspondingly, while the percentage of oxygen increased by 10%; moreover, trace amounts of phosphorus, sulphur and calcium appeared.

These results indicate the process of bed oxidation and dissolution as well as the sorption of solution components, including phosphorus. Sleiman et al. (2016) demonstrated that a sand bed with ZVI in its fragmented form was able to adsorb 152 mg P/g Fe during a several-day experiment. It is not clear how the adsorbed components affect the process efficiency. It can be assumed that both the blocking of electrolytic sites and the passivation of the material surface with the production of Fe oxides could have occurred (Mak et al. 2009). The adsorbed phosphate ions exhibit anti-corrosion properties and can inhibit the microelectrolysis process in the bed over a longer period (Wan et al. 2011; Lai et al. 2012).

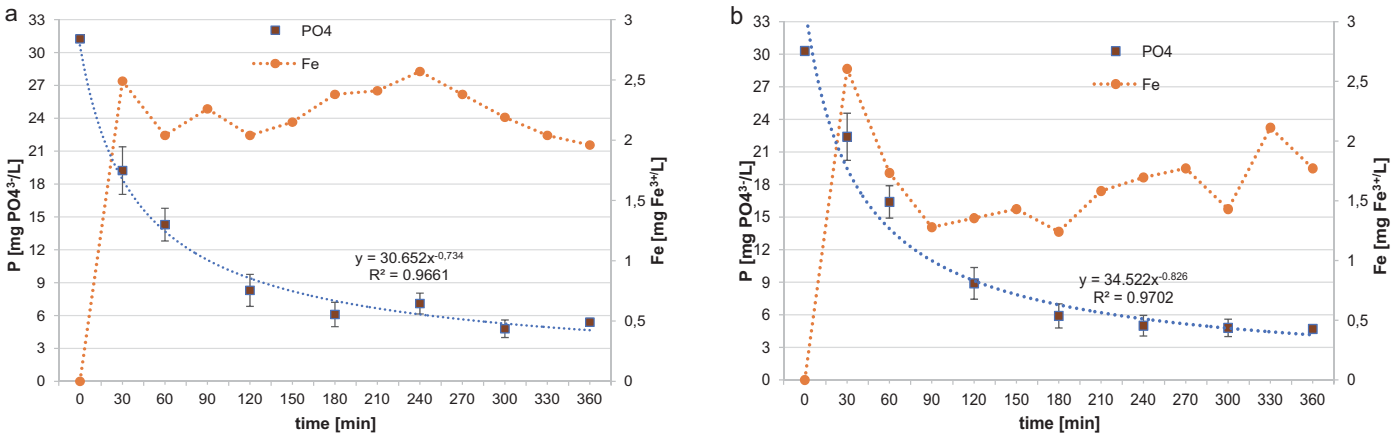

Fig. 4. Changes in the phosphate and total iron levels during the tests on reactors: 4a – MAC, 4b – AAC

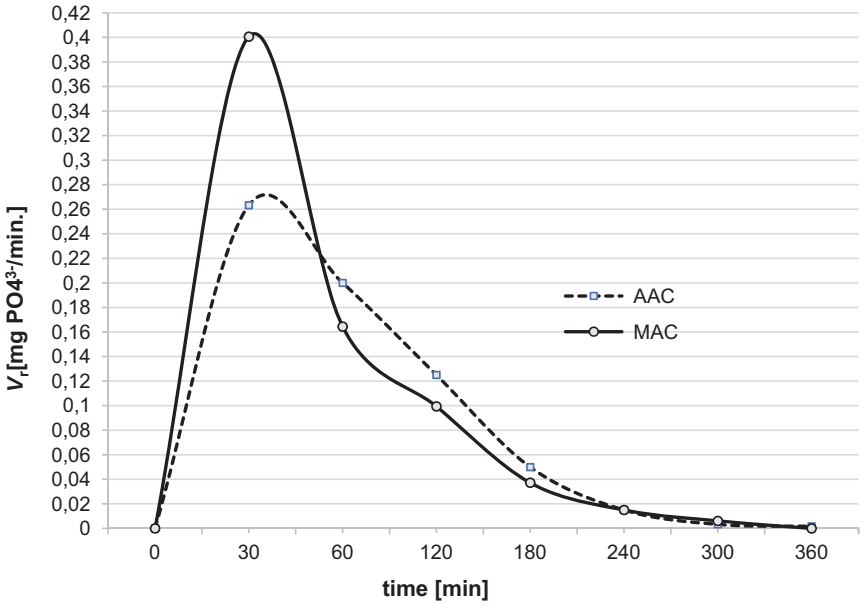

Fig. 5. Changes in the phosphate removal rate in reactors during the experiment

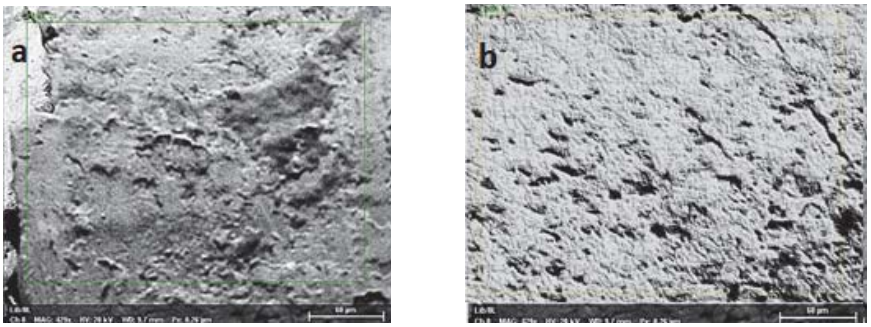

Fig. 6. Image of the MEL-bed filling surface: a – before, b – after action

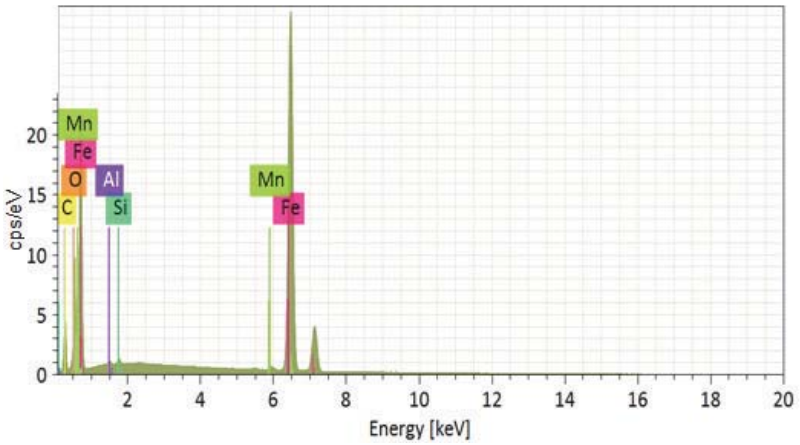

Fig. 7. Elementary analysis of the MEL-bed surface granule before electrolysis process

Table 2. The elementary composition of the surface granule layer of the bed before electrolysis

Spectrum	C	O	Al	Si	Mn	Fe	Cu
1	2	3	4	5	6	7	8
Content %	20.2 ± 0.08	5.85 ±1.09	0.22 ±0.06	0.18 ±0.03	7.13 ±0.34	69.09 ±4.73	0.22 ±0.00

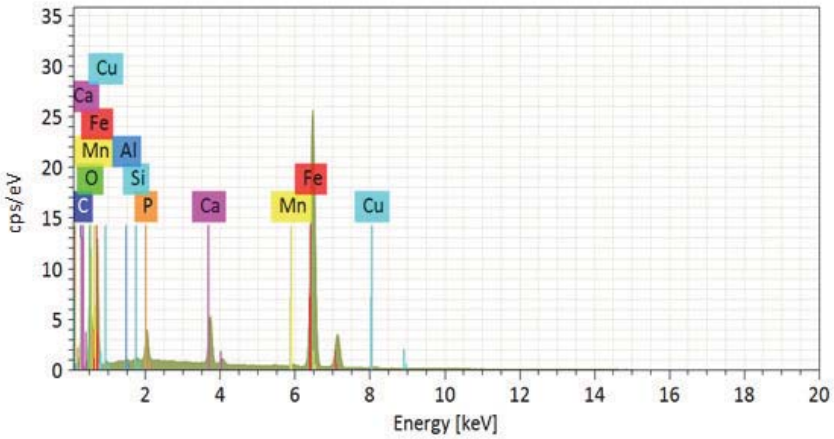

Fig. 8. Elementary analysis of the MEL-bed surface granule after electrolysis process

Table 3. The elementary composition of the surface granule layer of the bed after six hours of operation

Spectrum	C	O	Al	Si	P	S	Ca	Mn	Fe	Cu
1	2	3	4	5	6	7	8	9	1	2
Content %	14.01 ±4.79	15.5 ±7.24	0.22 ±0.15	0.15 ±0.07	0.88 ±1.11	0.12 ±0.03	2.23 ±1.99	6.6 ±1.2	60.22 ±11.63	0.11 ±0.14

Conclusions

The six-hour experiment demonstrated the efficiency of the microelectrolytic bed in the removal of phosphorus at a level of approx. 84% for both tested versions of the installation. The mechanical aeration method accelerated the treatment process in the initial phase, which lasted for up to 1 hour. In the first phase of the experiment in the MAC reactor, a higher Fe^{3+} concentration and the P removal rate were obtained. The maximum rate of phosphorus removal was noted in the 30th minute of the experiment and amounted to 0.40 mg PO_4^{3-}/min for the MAC and 0.26 mg PO_4^{3-}/min for the AAC. In the following minutes, the process effectiveness decreased almost to zero at the end of the test. Despite the differences in the course of phosphate removal kinetics in the initial phase of tests on both versions of the installation, the final effects of the treatment were comparable. The total weight of sludge after the experiment was greater for the AAC, which may indicate that the intense aeration in the MAC disturbs the aggregation and sedimentation processes. Based on the analyses performed, it can be concluded that phosphorus removal occurs due to the interaction with products of the corroding bed reactions in the solution and in the bed itself. The results suggest that the new installation is suitable for supporting wastewater treatment. The tested technology proved promising, although the experimental data need to be verified in terms of bed passivation during a long-term test and tested on a larger technical scale.

Acknowledgments

The results presented in this paper were obtained as part of a comprehensive study financed by the

University of Warmia and Mazury in Olsztyn, Faculty of Agriculture and Forestry, Department of Chemistry (grant No. 30.610.001-110).

References

Deng, Y., Englehardt, J.D., Abdul-Aziz, S., Bataille, T., Cueto, J., De Leon, O., Wright, M.E., Gardinali, P., Narayanan, A., Polar, J. & Tomoyuki, S. (2013). Ambient iron-mediated aeration (IMA) for water reuse, *Water Research*, 47, pp. 850–858, DOI: 10.1016/j.watres.2012.11.005.

El Samrani, A.G., Lartiges, B.S., Montarges-Pelletier, E., Kazpard, V., Barres, O. & Ghanbaja, J. (2004). Clarification of municipal sewage with ferric chloride: the nature of coagulant species, *Water Research*, 38, pp. 756–768, DOI: 10.1016/j.watres.2003.10.002.

Gromiec, M.J. & Gromiec, T.M. (2010). Controlling of eutrophication in aquatic environments, *Journal of Water and Land Development*, 14, pp. 29–35.

Gu, A.Z., Liu, L., Neethling, J.B., Stensel, H.D. & Murthy, S. (2011). Treatability and fate of various phosphorus fractions in different wastewater treatment processes, *Water Science and Technology*, 63 (4), pp. 804–810, DOI: 10.2166/wst.2011.215.

Lai, B., Zhou, Y. & Yang, P. (2012). Passivation of sponge iron and GAC in Fe^0/GAC mixed-potential corrosion reactor, *Industrial & Engineering Chemistry Research*, 51(22), pp. 7777–7785, DOI: 10.1021/ie203019t.

Lakshmanan, D., Clifford, D.A. & Samanta, G. (2009). Ferrous and ferric ion generation during iron electrocoagulation, *Environmental Science and Technology*, 43(10), pp. 3853–3859, DOI: 10.1021/es8036669.

Li, C., Ma, J., Shen, J. & Wang, P. (2009). Removal phosphate from secondary effluent with Fe^{2+} enhanced by H_2O_2 at nature pH/neutral pH, *Journal of Hazardous Materials*, 166, pp. 891–896, DOI: 10.1016/j.jhazmat.2008.11.111.

Libecki, B. (2018) Koagulator do oczyszczania ścieków (Coagulator for wastewater treatment) Patent Application, Polish Patent Office, application No: P.426089

Ma, L. & Zhang, W.-X. (2008). Enhanced biological treatment of industrial wastewater with bimetallic zero-valent iron, *Environmental Science and Technology*, 42, pp. 5384–5389, DOI: 10.1021/es801743s.

Mak, M.S.H., & Irene, M.C. (2009). Effects of hardness and alkalinity on the removal of arsenic(V) from humic acid-deficient and humic acid-rich groundwater by zero-valent iron, *Water Research*, 43, pp. 4296–4304, DOI: 10.1016/j.watres.2009.06.022.

Qin, Sh., Li, X., Zhang, T. & Ronga, W. (2011). Pretreatment of chemical cleaning wastewater by microelectrolysis process, *Procedia Environmental Sciences*, 10, pp. 1154–1158, DOI: 10.1016/j.proenv.2011.09.184.

Sarin, P., Snoeyink, V.L., Lytle, D.A. & Kriven, W.M. (2004). Iron corrosion scales: model for scale growth, iron release, and colored water formation, *Journal of Environmental Engineering*, 4, pp. 364–373.

Sleiman, N., Deluchat, V., Wazne, M., Mallet, M., Courtin-Nomade, A., Kazpard, V. & Baudu, M. (2016). Phosphate removal from aqueous solution using ZVI/sand bed reactor: Behavior and mechanism, *Water Research*, 99, pp. 56–65, DOI: 10.1016/j.watres.2016.04.054.

Smoczyński, L., Muńska, K.T., Kosobucka, M. & Pierożyński, B. (2014). Phosphorus and COD removal from chemically coagulated wastewater, *Environmental Protection Engineering*, 40(3), pp. 63–73.

Sterner, R.W. (2008). On the Phosphorus Limitation Paradigm for Lakes, *International Review of Hydrobiology*, 93, 4–5, pp. 433–445, DOI: 10.1002/iroh.200811068.

Sun, Y., Li, J., Huang, T. & Guan, X. (2016). The influeces of iron characteristics, operating conditions and solution chemistry on contaminants removal by zero-valent iron: A review, *Water Research,* 100, pp. 277–295, DOI: 10.1016/j.watres.2016.05.031.

Tarkowska-Kukuryk, M. (2013). Effect of phosphorus loadings on macrophytes structure and trophic state of dam reservoir on a small lowland river (eastern Poland), *Archives of Environmental Protection*, 39, 3, pp. 33–46, DOI: 10.2478/aep-2013-0029.

Wan, W., Pepping, T.J., Banerji, T., Chaudhari, S. & Giammar, D.E. (2011). Effects of water chemistry on arsenic removal from drinking water by electrocoagulation, *Water Research*, 45(1), pp. 384–392, DOI: 10.1016/j.watres.2010.08.016.

Wei, M.-Ch., Wang, K.-S., Hsiao, T.-E., Lin, I.-Ch., Wu, H.-J., Wu, Y.-L., Liu, P.-H. & Chang, S.-H. (2011). Effects of UV irradiation on humic acid removal by ozonation, Fenton and Fe^0/air treatment: THMFP and biotoxicity evaluation, *Journal of Hazardous Materials*, 195(15) pp. 324–331, DOI: 10.1016/j.jhazmat.2011.08.044.

Yang, X., Xue, Y. & Wang, W. (2009). Mechanism, kinetics and application studies on enhanced activated sludge by interior microelectrolysis, *Bioresources Technology*, 2009, 100(2), pp. 649–653, DOI: 10.1016/j.biortech.2008.07.035.

Yang, Z., Ma, Y., Liu, Y., Li, Q., Zhou, Z. & Ren, Z. (2017). Degradation of organic pollutants in near-neutral pH solution by Fe-C micro-electrolysis system. *Chemical Engineering Journal*, 315, pp. 403–414, DOI: 10.1016/j.cej.2017.01.042.

Yanhe, H., Han, L., Meili, L., Yimin, S., Cunzhen, L. & Jiaqing, Ch. (2016). Purification treatment of dyes wastewater with a novel

micro-electrolysis reactor, *Separation and Purification Technology*, 170, pp. 241–247, DOI: 10.1016/j.seppur.2016.06.058.

Yuan, S., Wu, Ch., Wan, J. & Lu, X. (2009). In situ removal of copper from sediments by a galvanic cell, *Journal of Environmental Management,* 90, 421–427, DOI: 10.1016/j.jenvman.2007.10.009.

Zou, H. & Wang, Y. (2017). Optimization of induced crystallization reaction in a novel process of nutrients removal coupled with phosphorus recovery from domestic wastewater, *Archives of Environmental Protection*, 43(4), 33–38, DOI: 10.1515/aep-2017-0037.

Usuwanie fosforu przez mikroelektrolizę i sedymentację w zintegrowanych urządzeniach

Streszczenie: W pracy zaprezentowano wyniki testów urządzenia z napowietrzanym złożem mikroelektrolitycznym (MEL-bed) i sedymentacją osadu. Urządzenie zaprojektowano w dwóch wersjach, różniących się sposobem napowietrzania. tj.: mechanical aerated coagulator (MAC) oraz automatically aerated coagulator (AAC). Eksperyment wykazał wysoką ok. 84% skuteczność usuwania fosforu z roztworu modelowego dla obydwu wersji. Korodujące złoże było źródłem żelaza w roztworze. Sposób napowietrzania miał wpływ na szybkość usuwania fosforu w początkowej fazie trwającej do 1 h oraz na procesy flokulacji i sedymentacji. Zaobserwowano zmiany fizyczne i chemiczne wypełnienia złoża MEL-bed.